Journal of Colloid and Interface Science 437 (2015) 10–16

Contents lists available at ScienceDirect

Journal of Colloid and Interface Science

www.elsevier.com/locate/jcis

Particle size- and number-dependent delivery to cells by layered double hydroxide nanoparticles

Haiyan Dong [a], Harendra S. Parekh [b,*], Zhi Ping Xu [a,*]

[a] Australian Institute of Bioengineering and Nanotechnology, The University of Queensland, Brisbane, QLD 4072, Australia
[b] Pharmacy Australia Centre of Excellence, School of Pharmacy, The University of Queensland, Brisbane, QLD 4102, Australia

ARTICLE INFO

Article history:
Received 6 August 2014
Accepted 8 September 2014
Available online 16 September 2014

Keywords:
Cellular delivery
Layered double hydroxide nanoparticles
Size dependent
Dose dependent

ABSTRACT

It is well known that delivery efficiency to cells is highly dependent on particle size and the administered dose. However, there is a marked discrepancy in many reports, mainly due to the inconsistency in assessment of various parameters. In this particular research, we designed experiments using layered double hydroxide nanoparticles (LDH NPs) to specifically elucidate the effect of particle size, dose and dye loading manner on cellular uptake. Using the number of LDH NPs taken up by HCT-116 cells as the indicator of delivery efficiency, we found that (1) the size of sheet-like LDH in the range of 40–100 nm did not significantly affect their cellular uptake; (2) cellular uptake of 40 and 100 nm LDH NPs was increased proportionally to the number concentration below a critical value, but remained relatively constant beyond the critical value; and (3) the effect of the dye loading manner is mainly dependent on the loading capacity or yield. In particular, the loading capacity is determined by the NP specific surface area. This research may be extended to a larger size range to examine the size effect, but suggests that it is necessary to set up a protocol to evaluate the effects of NP's physicochemical properties on the cellular delivery efficiency.

1. Introduction

Recent years have witnessed the enormous progress of nano-sized materials applied for drug/gene delivery, which include various polymeric nanoparticles (NPs), liposomes, metal (such as gold) and metal oxide (such as iron oxide, IO) NPs, mesoporous silica NPs (MSNs), carbon nanotubes (CNTs), layered double hydroxide (LDH) NPs, and their hybrids etc. [1–16].

It is well known that the physicochemical properties, such as NP size, shape, dose and surface charge, affect NP delivery efficacy. Of these characteristics, the particle size is a crucial factor which determines NP endocytosis pathway [17,18], uptake rate and efficiency [6,16,19–22], *in vitro* cytotoxicity [23–28], immune responses [27–30], and the final localisation [15,31,32]. Thus size-dependent uptake of various NPs has been intensively investigated and widely reported. For example, for organic NPs, some researchers claimed smaller NPs resulted in higher cellular uptake [22,33], while others reported an optimal size range for highest uptake [34–37]. Ross and Hui [38] even found linearly increasing cellular uptake of lipoplex in the size range of 35–2200 nm. For inorganic-based NPs, similar results were reported. Some researchers reported an optimal particle size for uptake of Au NPs, CNTs, and MSNs (~50 nm) [6,39–41], but some others found smaller Au, silica, and IO NPs had improved cellular uptake than larger ones in a certain size range [42–45].

Besides particle size, NP shape, on the other hand, also affects cellular uptake behaviour. Chithrani et al. [6] reported HeLa cell took up much more spherical Au NPs than rod-shaped Au NPs with a high aspect ratio. Jin et al. [40] found long and short SWNTs showed lower cellular uptake than those with the medium length. Choi and Choy's group studied the cellular uptake behaviours and mechanisms of LDH NPs (with sheet-like shape), finding 50 nm LDH NPs showed higher cellular uptake than 100–200 nm and 350 nm ones [46,47]. Recently we found 40 nm LDH NPs can carry 1–4 times more dsDNA than 100 nm ones at LDH:DNA mass ratio of 1:1 and 5:1, contributing to enhanced gene delivery [48,49].

In brief, the observations and conclusions differ from research groups, especially the particle size effect, being not so consistent and sometimes confused. This could be caused by several vague parameters without clear and consistent definition. The first one is NP size, which is normally characterised as the *Z*-average hydrodynamic diameter (measured by light scattering technology) [29,41,50] or the number average size (measured and statistically

* Corresponding authors. Fax: +61 7 3346 1887 (H.S. Parekh). Fax: +61 7 3346 3973 (Z.P. Xu).
E-mail addresses: h.parekh@uq.edu.au (H.S. Parekh), gordonxu@uq.edu.au (Z.P. Xu).

http://dx.doi.org/10.1016/j.jcis.2014.09.010
0021-9797/

calculated from TEM or SEM images) [6,28]. The second term is the dose of nanoparticle. Some have used the mass concentration while others used the particle number concentration. The third one is the delivery efficiency, often expressed as the NP number [6,16,43,51], the mass amount (pg/cell) [16,41], or the relative amount of labelled fluorescence dye [48,52] taken up by each cell. In addition, the difference in the shape and surface property from a variety of materials and surface modified functional groups may also cause the inconsistency. It is worth noting that the differing cell types used may also contribute to the inconsistency in determining the optimal particle size for the maximum cellular uptake efficiency.

Therefore, this particular research aimed to clearly elucidate effects of particle size (*Z*-average), dose (particle number concentration) and the dye loading (bulky or surface) of sheet-like LDH NPs on the uptake efficiency by HCT-116 cells. We found that (1) the cellular uptake efficiency of 40–50 nm NPs was similar to that of 90–100 nm NPs; (2) there was a critical particle number concentration, below which cellular uptake was in linear proportion to the particle number concentration, while beyond which cellular uptake was not improved; (3) dye loading on the surface may also affect cellular uptake depending on the surface loading capacity.

2. Experimental

2.1. LDH NPs preparation

Small LDH (sLDH) NPs were prepared by a non-aqueous precipitation method [48,49]. Briefly, 10 mL methanol (Fluka, ⩾99.0%) solution containing 6 mmol of $Mg(NO_3)_2{\cdot}6H_2O$ and 2 mmol of $Al(NO_3)_3{\cdot}9H_2O$ (Fluka, >99.0%) was added drop-wise to a 40 mL solution of methanol containing 16 mmol NaOH (Fluka, >97.0%, pellets) under vigorous stirring. The precipitate slurry was collected via centrifugation, then redispersed in 40 mL fresh methanol and transferred to a Teflon®-lined autoclave for heat-treatment at 100 °C for 4 h. The final LDH slurry was collected and manually dispersed in 40 mL of deionised water after washing twice with deionised water. This dispersion resulted in a homogeneous sLDH suspension after 4–6 days with a sLDH mass concentration of 6–7 mg/mL.

Large LDH (L-LDH) NPs were synthesised by mixing 10 mL of aqueous solution containing 3.0 mmol of $MgCl_2{\cdot}6H_2O$ and 1.0 mmol of $AlCl_3{\cdot}6H_2O$ (Sigma–Aldrich, 99.0–102.0%) with 40 mL of 0.15 M NaOH solution and vigorously stirred for 10 min at room temperature [53,54]. The LDH slurry was collected by centrifugation, washed twice with deionised water (40 mL), and then resuspended in deionised water (40 mL). The suspension was then transferred to a Teflon®-lined autoclave and hydrothermally treated at 100 °C for 16 h. The suspension contained approximately 4 mg/mL of homogeneously dispersed L-LDH NPs.

Both small and large LDH-FITC NPs were prepared by the ion-exchange method. Here, FITC (fluorescein isothiocyanate isomer I, Sigma–Aldrich) sodium solution (0.05 or 0.01 mmol) was mixed with 1 mmol of either sLDH or L-LDH slurry and then shaken on a reciprocal shaker for 1 h. After ion-exchange, the unchanged FITC and residual sodium nitrate or sodium chloride ($NaNO_3$/NaCl) were separated. The collected slurry was then redispersed in deionised water and subjected to 2–4 h of hydrothermal and sterilisation treatment.

All NP sizes were determined by dynamic light scattering (DLS, Zetasizer Nano ZS, Malvern Ltd). The *Z*-average size of sLDH was found to be ~40 nm (~54 nm for sLDH-FITC), while L-LDH measured ~100 nm (~90 nm for L-LDH-FITC).

2.2. Suspension stability test

LDH NPs were diluted by complete cell culture media (10% *v/v*) of foetal bovine serum (Gibco®) mixed with Dulbecco's Modified Eagle Medium (DMEM, with L-glutamine and 4.5 g/L of glucose, Gibco®)) at desired concentrations, and then particle size distribution of the suspension mixture was measured using the Zetasizer.

2.3. Nucleic acid loading and agarose gel electrophoresis

Nucleic acids were loaded on LDH NPs by mixing LDH suspension with nucleic acid solution at the LDH:dsDNA mass ratios of 2:1, 5:1, 10:1, 20:1, and 40:1. A 2.5% agarose (molecular grade, Bioline) gel with Gel-Red (Invitrogen™) stain was made and then nucleic acids with/out LDH for binding were loaded in the wells. For each well, 260 ng double stranded DNA (dsDNA DCC1, Geneworks) was used. Gel was imaged by a Bio-Rad imaging system after a run at 90 V for 45 min in TBE (Tris/Borate/EDTA, Invitrogen™) buffer.

2.4. Cellular uptake

HCT-116 cells were seeded in 6-well plates at density of 1×10^5 cells per well in 2 mL complete cell culture media. After 24 h of incubation, cell culture media was replaced by 1 mL of fresh media with/out desired concentrations of LDH-FITC NPs or LDH-DNA-Cy3 NPs (40 nM DNA was used). At different time points after further incubation (from 15 min to 8 h), the culture media was removed, and cells were washed twice with PBS buffer (Gibco®) and then detached from the plates by trypsin–EDTA (Gibco®). The cells were washed twice with PBS buffer and then fixed in a certain volume of 2% PFA (paraformaldehyde, Chemsupply) before measurement by flow cytometry (BD Accuri™ C6 Flow Cytometer System, band pass filter 530/30 for detecting FITC, 585/40 for detecting Cy3, 10,000 cells were counted). All treatments were performed for three different batches in duplicate. Data are presented as the mean ± SEM (standard error of the mean).

3. Results

3.1. Suspension stability of sLDH and L-LDH NPs

As shown in Fig. 1A, sLDH and L-LDH NPs were well dispersed in water, having a hydrodynamic diameter ranging from 10 to 100 nm with a *Z*-average size of 40 nm, and from 40 to 250 nm with the *Z*-average size of 100 nm, respectively. The *Z*-average size here is the intensity weighted mean hydrodynamic diameter of particles (more details can be referred to Malvern Instruments Frequently Asked Question "What is the Z-average"). Both sLDH and L-LDH NPs have a zeta potential of ~40 mV, which is in agreement with earlier reports for LDH [48,54,55].

When LDH NPs were diluted in complete cell culture media, both sLDH and L-LDH NPs aggregated, and this was found to be concentration- and size-dependent. As shown in Fig. 1B, when the sLDH NP suspension was diluted to a concentration range of 100–800 μg/mL, sLDH formed aggregates with a *Z*-average size of 200–450 nm. Applying the same concentration range to L-LDH NPs, they also aggregated but to a lesser extent, with a *Z*-average size of 180–300 nm. The *Z*-average size (74 and 107 nm) was in close agreement with that in the original suspension for both sLDH and L-LDH when they were further diluted to 40 μg/mL (Fig. 1B). The aggregation may affect the cellular uptake as Andersson et al. [56] found NP uptake was strongly dependent on the agglomeration size, not the primary particle size. This proved serendipitous as the concentration of LDH NPs used in cellular uptake

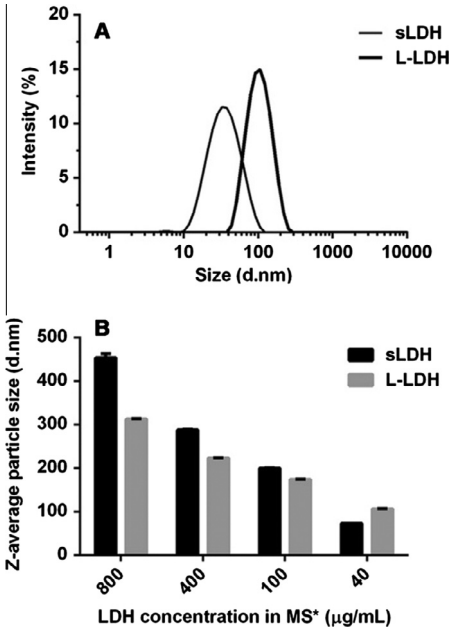

Fig. 1. Particle sizes of sLDH and L-LDH NPs in water and complete cell culture media at different concentrations (*MS = medium + serum, i.e. the complete cell culture medium).

studies did not typically exceed 40 μg/mL so as to circumvent unwanted NP aggregation.

Particle aggregation was more pronounced with sLDH in the culture media and this could be attributed to their relative dimensions compared to L-LDH. sLDH possesses a surface area 2.5 times that of L-LDH NPs, and thus its capacity to adsorb proteins (a key driver of aggregation) present in cell culture media is also considered to be 2.5-fold greater than L-LDH. Upon lowering the NP concentration sufficiently (i.e. to <40 μg/mL), sLDH and L-LDH NPs adsorb protein until they reach a relative state of equilibrium, at which point their surface properties are dictated by adsorbed proteins such that aggregation is suppressed. That said, at high NP concentrations, one can expect to reach a point where all available proteins are adsorbed by the NPs, and this triggers surface adsorbed proteins to reach out and form protein-bridges with neighbouring particles, resulting in aggregation. This latter phenomenon is likely to be more of an issue with sLDH, as L-LDH possesses a smaller surface area and so is able to accommodate far less protein.

3.2. Gene loading

Fig. 2 shows the electrophoretic mobility of dsDNA loaded onto LDH NPs at increasing LDH:dsDNA mass ratios. The first lane for each gel represents a 21–25 bp dsDNA marker, and the bright bands towards the bottom of the gels are free dsDNA. As can be seen in Fig. 2A, sLDH NPs completely immobilised dsDNA at the mass ratio of ⩾5:1 in water, while at 2:1 some free dsDNA was present. Similarly, L-LDH NPs completely bound dsDNA at the mass ratio of ⩾10:1 in water, while the binding was not complete at 5:1 (Fig. 2C). This difference can again be attributed to the particle size as the larger surface area of sLDH NPs can accommodate a greater load of dsDNA as compared to L-LDH NPs at the equivalent mass concentration.

When the LDH-dsDNA complexes were assessed in complete cell culture media, electrophoretic studies revealed less dsDNA immobilised (Fig. 2B and D) than that in water (Fig. 2A and C). In the complete cell culture media, only at mass ratios of 20:1 and 40:1 was dsDNA observed to be completely bound by both sLDH and L-LDH NPs. However, the surface area of the respective NPs again yielded subtle differences in binding with dsDNA at the lower (e.g. 5:1) mass ratios.

As alluded to earlier, the significant differences in mass ratios necessary to completely immobilise dsDNA in water versus complete cell culture media can once again be attributed to the competitive adsorption of proteins (in serum) onto the respective NP surfaces. This competition results in a relatively higher mass of LDH NPs needed to fully complex dsDNA in complete cell culture media, and is a phenomenon seen with other vector-DNA complexation studies [57].

3.3. Cellular uptake kinetics of LDH-FITC NPs

3.3.1. Dose-dependent uptake

We first tested the cellular uptake of FITC-labelled NPs at different LDH concentrations by HCT-116 cells. The FITC loading capacity within both types of LDH NPs was comparable, being 5% of all intercalated anions (denoted as LDH-5%FITC). We found that >99% of cells were FITC-positive after incubation with either sLDH-5%FITC or L-LDH-5%FITC at 4 h, and across the concentrations measured (2.5–20 μg/mL) (Fig. 3A and B). The mean fluorescence intensity of cells treated with sLDH-5%FITC at these concentrations did not change (⩾5.0 μg/mL), indicating that cellular uptake was saturated under these conditions. Our previous confocal images have confirmed that hexagonal LDH NPs are taken up by various cell types and are mostly located in the cytoplasm [48,54,58,59].

In sharp contrast, the mean fluorescence intensity of cells treated with L-LDH-5%FITC exhibited increasing fluorescence intensity as the LDH concentration was raised (Fig. 3C); this reveals that the cellular uptake of L-LDH-5%FITC continued under the same conditions albeit at a declining rate, indicating the saturated particle concentration for L-LDH-5%FITC is most likely in the region of 20 μg/mL. For sLDH, at the concentration of 1.4 μg/mL, the mean fluorescence intensity was quite low, showing a strong dependence on the sLDH mass concentration, similar to the dependence seen by L-LDH at 2.5–20 μg/mL (Fig. 3C). Choy et al. [11] also found dose dependent uptake of LDH-FITC NPs by NIH 3T3 cells in the test concentration range (<45 μM). Li et al. [50] reported concentration dependent uptake of 65 nm CO_3LDH-FITC by NSC 34 cells in the concentration range of 6.25–100 μg/mL, where FITC was adsorbed onto the surface of CO_3-LDH instead of intercalated into the interlayers.

3.3.2. Time-dependent uptake

To explore LDH-5%FITC cell uptake kinetics, time-dependent uptake of small and large LDH-5%FITC at 1.4 and 10.0 μg/mL was investigated. Fig. 4A shows that almost all cells treated with 1.4 μg/mL of L-LDH-5%FITC were FITC-positive after ⩾2 h, although the mean FITC fluorescence intensity kept increasing with incubation time (Fig. 4C). In comparison, only 25–35% cells were FITC-positive with the mean FITC fluorescence intensity nearly constant when treated with sLDH-FITC at this concentration for ⩾2 h. Of note was that the mean fluorescence intensity of cells treated with L-LDH was 15–20 times that of sLDH, after 2–8 h of incubation.

In the case of 10 μg/mL of FITC-labelled LDH NPs, almost all cells were FITC-positive upon treatment with both small and large LDH-5%FITC NPs (Fig. 4B) after 4 h of incubation. During the 15 min–4 h incubation window L-LDH-5%FITC led to a marginally higher percentage of FITC-positive cells. This is comparable to what Li et al. [55] reported, where 60–70% of positive cells were observed after incubating MDDC cells with 20 μg/mL FITC-labelled LDH NPs (hydrodynamic number size ~60 nm). The mean FITC intensity continuously increased during the whole uptake process

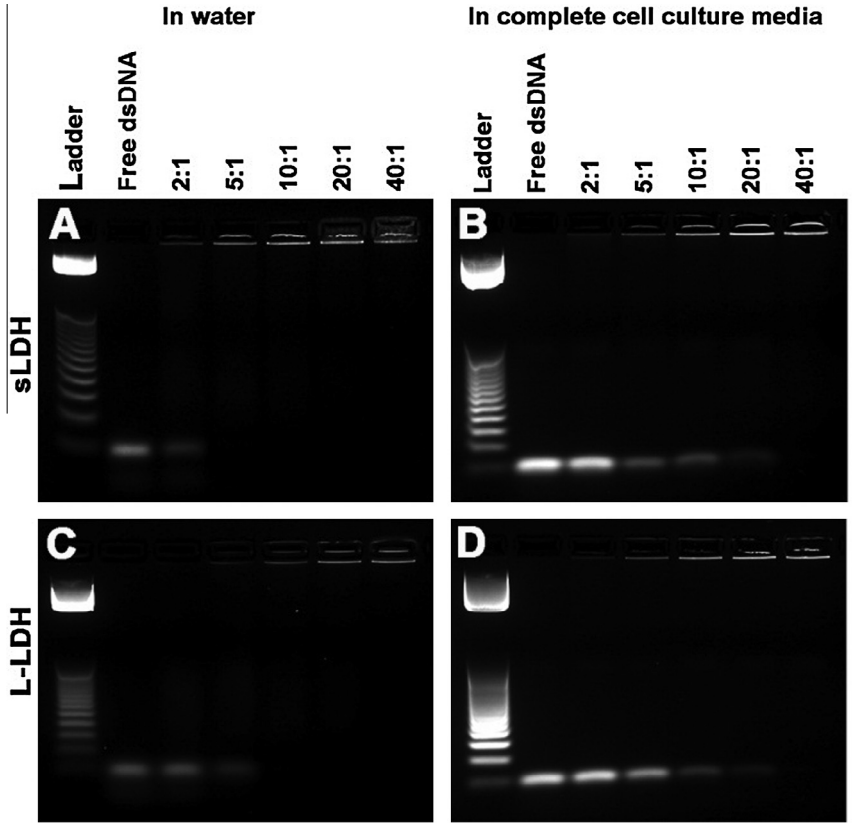

Fig. 2. Electrophoretic study comparing loading of dsDNA into sLDH and L-LDH NPs in the presence of water (A and C) and complete cell culture media (B and D) at increasing mass ratios.

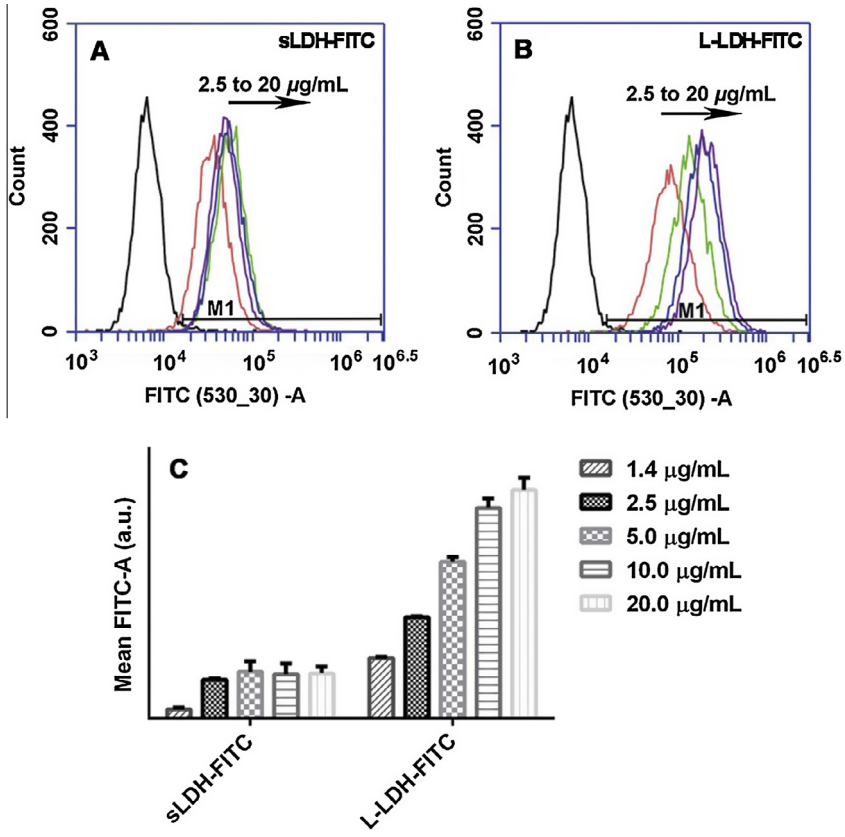

Fig. 3. Cellular uptake of LDH-5%FITC NPs at different concentrations by HCT-116 cells.

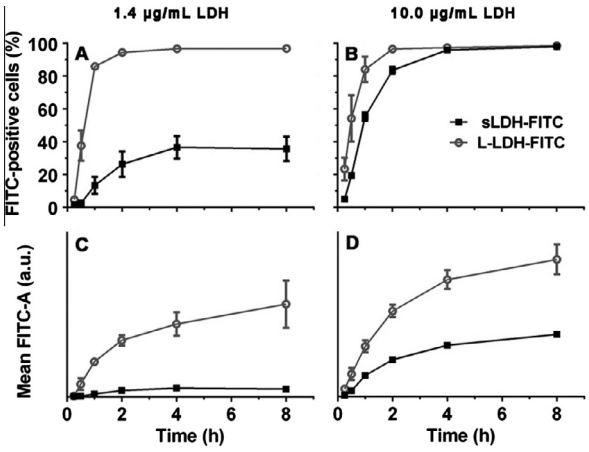

Fig. 4. Time course cellular uptake of LDH-5%FITC NPs at equivalent mass concentration by HCT-116 cells.

with both sets of NPs (Fig. 4D). Such a time-dependent uptake of LDH-FITC NPs by NIH 3T3 cells was also reported by Choy et al. [11] Interestingly, the mean FITC fluorescence intensity of the cells treated with 10 μg/mL of L-LDH-5%FITC appeared to be 2–3 times that of the cells treated with 10 μg/mL of sLDH-FITC at each time point.

3.3.3. Particle size-dependent uptake

To elucidate specifically the role of NP size on the rate and efficiency of cellular uptake, we particularly prepared L-LDH NPs containing 1% FITC (L-LDH-1%FITC, ~90 nm) and compared the cellular uptake at 20 μg/mL of L-LDH-1%FITC and 4 μg/mL of sLDH-5%FITC (both being close to saturated particle concentration as discussed earlier). In this series of experiments, each FITC-labelled NP contained an equivalent amount of FITC and the NP number concentration was also the same. Thus, assessment of cellular uptake efficiency would be reflected purely from a NP-size perspective. As shown in Fig. 5, similar FITC-positive cell percentage and mean FITC intensity were observed in both cases. The subtle difference is that cellular uptake efficiency equilibrated after 2 h of incubation with sLDH-FITC, while L-LDH-FITC NP uptake kept increasing over the same period, as measured by the percentage of FITC-positive cells and mean FITC fluorescence intensity. This probably reflected a more rapid uptake of sLDH-FITC NPs before 4 h, but sustained and continuous uptake of L-LDH-FITC NPs after 4 h. Rapid internalisation of 50 and 100 nm spheric NPs compared to 200 nm ones was also reported by Rejman et al. [18]. More interestingly, the continuous uptake of larger NPs was also observed and reported for viral NPs [60], polyplexes [61], and lipoplexes [62].

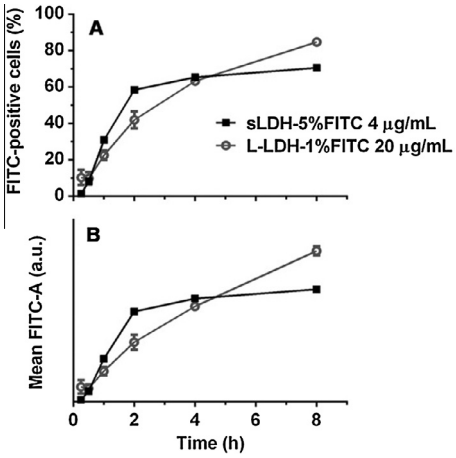

Fig. 5. Time course cellular uptake of sLDH-5%FITC and L-LDH-1%FITC by HCT-116 cells (at identical particle concentration and FITC loading).

3.4. Cellular uptake of LDH-DNA

We next investigated the cellular uptake of LDH-DNA complexes, where DNA was predominantly adsorbed on the LDH NP surface [48,59]. The loading capacity of DNA onto LDH was determined by varying the LDH: DNA mass ratios, as discussed previously (Fig. 2). Based on the observations in Fig. 2, we chose two LDH:DNA mass ratios, the first of which reflected incomplete LDH-DNA complexation (5:1) while the second reflected complete complexation (40:1), irrespective of NP size. The time-dependent cellular uptake of both sets of LDH NPs with DNA-Cy3 is presented in Fig. 6.

At the mass ratio of 5:1 (40 nM DNA-Cy3 and 1.4 μg/mL sLDH), the percentage of Cy3-positive cells quickly increased to 60% after just 2 h incubation, and then slowly increased to 80% over the next 6 h. However, in the case of L-LDH-DNA-Cy3, the percentage of Cy3-positive cells increased steadily over the entire incubation period, reaching a mere 20% after 8 h incubation (Fig. 6A). The mean Cy3 fluorescence intensity followed a similar trend (Fig. 6C). Our findings are consistent with our previous observation in HEK-293T cells [49], suggesting that partial complexation of DNA by L-LDH NPs at this mass ratio is detrimental to gene delivery efficiency. This observation seems to be similar to the report by Elbakry et al. [63] that far more DNA molecules were delivered to one cell by 20 nm Au NPs than 80 nm ones.

At the mass ratio of 40:1 (40 nM DNA-Cy3 and 11 μg/mL LDH), treatment with sLDH and L-LDH led to a similar population of Cy3-positive cells after 2 h of treatment. Prior to this time frame, a higher percentage of Cy3 positive cells was seen with sLDH (Fig. 6B). The mean Cy3 fluorescence intensity of cells treated with sLDH was twice that of cells treated with L-LDH after 1–8 h of incubation (Fig. 6D), which indicates that sLDH is able to transport twice the load of DNA as L-LDH, at this mass ratio. This observation appears to be consistent with the following reports: more rapid internalisation of smaller DNA/PEI complexes by K562 cells [64], and smaller PLGA NPs by COS-7 and HEK-293 cells [65].

4. Discussion

The ease by which therapeutic nanoparticles (e.g. gene-carrier systems) are taken up by their target cell population will directly

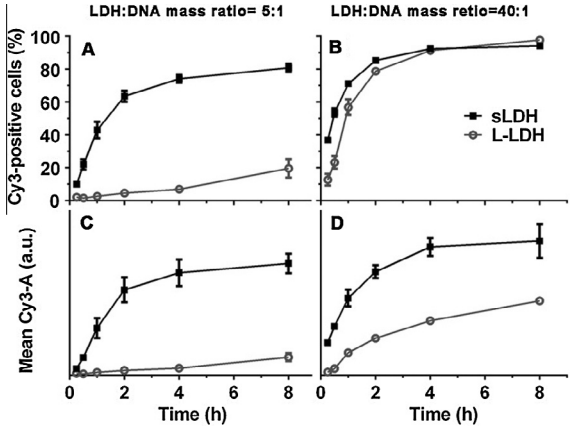

Fig. 6. Time course cellular uptake of LDH-DNA-Cy3 by HCT-116 cells.

impact on quantifiable outcomes which ultimately dictate their 'efficiency', such as the rate and intensity of transfection/fluorescence measured across a population of cells. With this in mind, the key concepts underlying this work presented here aimed to explore and decipher the effects of the LDH particle size, LDH particle number concentration and dye/gene loading by LDH on cellular delivery efficiency, using sLDH and L-LDH as our key NP comparators.

4.1. Effect of LDH-NP size on cellular delivery efficiency

To specifically examine the effect of LDH particle size on delivery efficiency, we fixed the particle number concentration of either sLDH or L-LDH particles. Since each L-LDH-FITC particle (90 nm) is about 5 times ($90^3/54^3 = 4.6$) larger from a volume perspective than each sLDH-FITC particle (54 nm), we employed 4 μg/mL sLDH-5%FITC and 20 μg/mL L-LDH-1%FITC to ensure the presence of a similar particle number concentration alongside an identical load of FITC in each LDH particle. In such a cellular uptake test, the FITC fluorescence intensity observed for each NP type when delivered to a population of cells directly reflects the impact of the particle size on uptake by HCT-116 cells.

Under these 'identical' conditions, HCT-116 cells were shown to internalise a similar amount of FITC irrespective of whether the vector being used was sLDH or L-LDH (Fig. 5). The only subtle difference was that the cellular uptake of sLDH NPs was seen to be complete in the first 2 h, while L-LDH NPs showed a steady and continual uptake over up to 8 h. Thus, this work shows that the rate of cellular uptake in terms of the particle number was comparable for the 54 nm (sLDH) and 90 nm (L-LDH) NPs. It is reported that internalisation of NPs less than 200 nm involves the clathrin-mediated endocytotic pathway [17,18,66,67]; thus sLDH-FITC (~54 nm) and L-LDH-FITC (~90 nm) used in this work entered HCT-116 cells through the same pathway. That would be the reason why sLDH-FITC and L-LDH-FITC resulted in similar uptake regardless of the particle size difference. This result is consistent with recent *in vitro* and *in silico* correlation studies where NPs ranging in size from 50 to 100 nm were found to be optimal for cellular delivery [34]. It is also in partial agreement with a cluster of earlier studies where *ca.* 50 nm NPs were more efficiently internalised by a range of cell types [6,46].

Clearly, the cellular uptake rate of L-LDH from the particle 'mass' perspective is about 5 times that of sLDH as the volume of one L-LDH particle is nearly 5 times that of one sLDH particle. This translates to the fact that if sLDH-5%FTIC and L-LDH-5%FITC NPs are delivered at an equivalent particle number concentration in cellular uptake studies, the mean FITC fluorescence intensity of HCT 116 cells treated by L-LDH-5%FITC would be expectedly 5 times that treated by sLDH-5%FTIC, which is really shown by the data in Fig. 3. The mean fluorescence intensity of cells treated with 10.0–20.0 μg/mL of L-LDH-5%FITC was truly about 5 times that of cells treated with 2.5–5.0 μg/mL of sLDH-5%FITC, where the particle number concentration in the two cases was approximately the same.

4.2. Effect of the LDH particle number concentration on cellular delivery efficiency

As shown in Fig. 3C, the amount of FITC delivered by sLDH remained largely unchanged at mass doses $\geqslant$5.0 μg/mL, while it increased substantially at the lower mass dose range of 1.4–5.0 μg/mL. Similarly, the amount of FITC delivered by L-LDH increased steadily at a mass dose from 1.4 to 20.0 μg/mL while the increase was minimal from 10.0 to 20.0 μg/mL. It appears that cellular uptake of NPs is dose dependent below a critical mass concentration, while cellular uptake of NPs reaches a plateau at or beyond the critical mass concentration. In the current two cases, the critical mass concentration of sLDH and L-LDH is in the region of 5 and 20 μg/mL, respectively. Interestingly, the corresponding critical particle number concentration in these two cases is very similar, at approximately 1.0×10^{10} number/mL, which is also supported by the data shown in Fig. 7. The uptake curves are quite similar for sLDH and L-LDH NPs, with a similar critical particle number concentration. Clearly, cellular uptake in terms of the LDH particle number is almost linearly dependent on the particle number concentration below the critical number concentration (1.0×10^{10} number/mL). Beyond this critical value, cellular uptake does not improve. Chithrani et al. [6] have also reported dose-dependent phenomena, and moreover, their critical NP number concentration was estimated to be 0.3×10^{10} number/mL for 50 nm Au NPs based on the data provided, which is in close agreement with our critical number concentration. Of course, the critical number concentration of NPs could also be dependent on the cell type and confluency.

As depicted in Fig. 4D, the amount of FITC delivered by L-LDH was approximately twice that of sLDH after incubation for 1–8 h at the same mass concentration (10 μg/mL). From this we can infer that sLDH particle numbers taken up by HCT-116 cells was about 2.5 times that of L-LDH, although the number concentration of sLDH particles was 5 times that of L-LDH particles. This uptake rate of sLDH in terms of the particle number is less than that expected (5 times), which could be due to the fact that the mass concentration of sLDH (10 μg/mL) is beyond the critical mass concentration value (5 μg/mL) while that of L-LDH is below. Therefore, the rate of cellular uptake of L-LDH is relatively slower in this instance.

4.3. Effect of surface/internal-bulk loading on cellular delivery efficiency

The cellular delivery efficiency can be also determined by the manner of loading on/into the respective NPs. For example, the amount of DNA-Cy3 delivered by sLDHs was 2–3 times that delivered by L-LDH (Fig. 6D). This is in sharp contrast to the results in Fig. 4D where the amount of FITC delivered by sLDH was 2 times less than that delivered by L-LDH, which reflects the impact of loading style. It is important to note that DNA was loaded onto LDH in a manner different from FITC, where FITC was intercalated between the interlayers (bulk way), but DNA predominantly adsorbed onto the surface of LDH NPs (surface way). Due to the differences in loading sites on the NP, FITC loading could be controlled through percentage of interlayer anion exchange and correlated with the LDH NP volume, while DNA loading amount was correlated with the LDH surface area.

At the equivalent mass concentration, sLDH with the *Z*-average size of 40 nm has a surface area 2.5 times that of L-LDH with the *Z*-average diameter size of 100 nm. From a loading perspective,

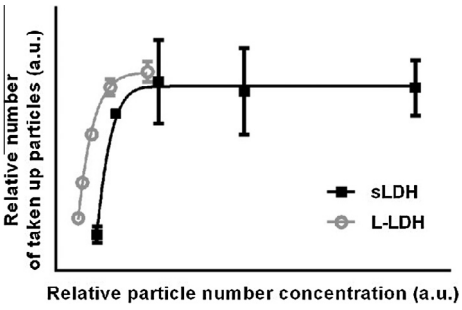

Fig. 7. Replot of normalised particle number concentration and particle number taken up by cells based on the data in Fig. 3, including sLDH and L-LDH.

this means that sLDH is able to carry 2.5 times the load of DNA as that of L-LDH, at the equivalent mass concentration. This may explain why sLDH bound almost all DNA at the LDH:DNA mass ratio of 2:1 (Fig. 2A), while a mass ratio of 5:1 was necessary in the case of L-LDH (Fig. 2C). This may further reflect that the contribution of unassociated DNA at the mass ratio of 5:1 was much lower from sLDH (~10%) than from L-LDH (~50%) in the culture media (Fig. 2B and D). Cebrián et al. [68] also found 6 nm PEI-coated Au NPs can load higher quantities of DNA than equivalent mass of 70 nm Au-PEI NPs because of the larger external surface area per unit mass. The incomplete complexation of DNA-Cy3 observed with L-LDH at 5:1 in culture media would be expected to reduce the cellular delivery of DNA-Cy3 to 50% of that using sLDH at the same particle number concentration.

Aside from the effect of incomplete complexation, the observed difference in the delivery efficiency of DNA-Cy3 may largely be attributed to LDH particle number concentration changes. Here, as the L-LDH particle number concentration (1.4 and 11 μg/mL) was well below the critical value, cellular uptake of DNA-Cy3 would increase in proportion to the particle number concentration. In comparison, sLDH NP number concentration at 1.4 μg/mL is below the critical value while 11 μg/mL is well over the critical value, so cellular uptake would increase less than in a proportional manner. This understanding, together with the loading yield, goes some way towards explaining why the amount of DNA-Cy3 delivered by sLDH was 10–15 times higher than that of L-LDH at the mass ratio of 5:1, decreasing to about 2–3 times higher at the mass ratio of 40:1 (Fig. 6C and D).

5. Conclusions

The cellular uptake of LDH NPs is highly dependent on its particle number concentration regardless of particle size in the range of 40–100 nm. Under the critical particle number concentration, cellular uptake was in linear proportion to the particle number concentration, while above this critical value, the cellular uptake was not further improved. This research further found that the size of sheet-like LDH particles in the range of 40–100 nm could not significantly affect the cellular uptake in terms of the particle number, and that the surface loading capacity of LDH NPs may significantly affect the delivery efficiency.

Acknowledgments

The authors gratefully acknowledge the financial support from ARC Discovery Project Grants (DP0879769 and DP120104792) and ARC Future Fellowship (FT120100813). Thanks also go to Dr. Wenyi Gu from Australian Institute for Bioengineering & Nanotechnology and Dr. Jiezhong Chen from School of Biomedical Sciences for providing the cell line.

References

[1] R. Gref, Y. Minamitake, et al., Science 263 (1994) 1600–1603.
[2] O. Boussif, F. Lezoualch, et al., Proc. Natl. Acad. Sci. USA 92 (1995) 7297–7301.
[3] H. Liu, Y. Wang, et al., Biomaterials 35 (2014). pp.
[4] J. Hughes, P. Yadava, et al., Liposomal siRNA delivery, in: V. Weissig (Ed.), Liposomes: Methods and Protocols, Pharmaceutical Nanocarriers, vol. 1, Humana Press, 2009, pp. 445–459.
[5] N.L. Rosi, D.A. Giljohann, et al., Science 312 (2006) 1027–1030.
[6] B.D. Chithrani, A.A. Ghazani, et al., Nano Lett. 6 (2006) 662–668.
[7] A.K. Gupta, M. Gupta, Biomaterials 26 (2005) 3995–4021.
[8] X. Huang, X. Teng, et al., Biomaterials 31 (2010) 438–448.
[9] Y. Gao, Y. Chen, et al., ACS Nano 5 (2011) 9788–9798.
[10] N.W.S. Kam, T.C. Jessop, et al., J. Am. Chem. Soc. 126 (2004) 6850–6851.
[11] J.-H. Choy, S.-Y. Kwak, et al., Angew. Chem. Int. Ed. 39 (2000) 4041–4045.
[12] J. Li, Y.-C. Chen, et al., J. Controlled Release 142 (2010) 416–421.
[13] S.C. Rizzi, D.T. Heath, et al., J. Biomed. Mater. Res. 55 (2001) 475–486.
[14] S.B. Hartono, W. Gu, et al., ACS Nano 6 (2012) 2104–2117.
[15] E. Oh, J.B. Delehanty, et al., ACS Nano 5 (2011) 6434–6448.
[16] J. Huang, L. Bu, et al., ACS Nano 4 (2010) 7151–7160.
[17] I. Canton, G. Battaglia, Chem. Soc. Rev. 41 (2012) 2718–2739.
[18] J. Rejman, V. Oberle, et al., Biochem. J. 377 (2004) 159–169.
[19] S. Zhang, J. Li, et al., Adv. Mater. 21 (2009) 419–424.
[20] F. Osaki, T. Kanamori, et al., J. Am. Chem. Soc. 126 (2004) 6520–6521.
[21] S. Reichert, P. Welker, et al., Small 7 (2011) 820–829.
[22] Y. Hu, J. Xie, et al., J. Controlled Release 118 (2007) 7–17.
[23] Y. Yuan, C. Liu, et al., Biomaterials 31 (2010) 730–740.
[24] S. Xiong, S. George, et al., Arch. Toxicol. 87 (2013) 1075–1086.
[25] A.R. Gliga, S. Skoglund, et al., Part. Fibre Toxicol. 11 (2014). pp. 11-11.
[26] S.-J. Choi, J.-M. Oh, et al., J. Nanosci. Nanotechnol. 8 (2008) 5297–5301.
[27] X. Wang, X. Li, et al., Acta Biomater. 9 (2013) 7480–7489.
[28] S. Kim, W.-K. Oh, et al., Biomaterials 32 (2011) 2342–2350.
[29] W.-K. Oh, S. Kim, et al., ACS Nano 4 (2010) 5301–5313.
[30] K. Niikura, T. Matsunaga, et al., ACS Nano 7 (2013) 3926–3938.
[31] S. Ohta, P. Shen, et al., J. Mater. Chem. 22 (2012) 10631–10638.
[32] S. Schubbe, C. Schumann, et al., Chem. Mater. 24 (2012) 914–923.
[33] S. Bhattacharjee, D. Ershov, et al., Part. Fibre Toxicol. 9 (2012). pp.
[34] A. Xu, M. Yao, et al., Int. J. Nanomed. 7 (2012) 3547–3554.
[35] K.Y. Win, S.S. Feng, Biomaterials 26 (2005) 2713–2722.
[36] S.A. Kulkarni, S.-S. Feng, Pharm. Res. 30 (2013) 2512–2522.
[37] M. Massignani, C. LoPresti, et al., Small 5 (2009) 2424–2432.
[38] P.C. Ross, S.W. Hui, Gene Ther. 6 (1999) 651–659.
[39] W. Jiang, B.Y.S. Kim, et al., Nat. Nanotechnol. 3 (2008) 145–150.
[40] H. Jin, D.A. Heller, et al., ACS Nano 3 (2009) 149–158.
[41] F. Lu, S.-H. Wu, et al., Small 5 (2009) 1408–1413.
[42] Y. Shan, S. Ma, et al., Chem. Commun. 47 (2011) 8091–8093.
[43] E.C. Cho, L. Au, et al., Small 6 (2010) 517–522.
[44] L. Tang, T.M. Fan, et al., ACS Nano 6 (2012) 3954–3966.
[45] L. Matuszewski, T. Persigehl, et al., Radiology 235 (2005) 155–161.
[46] S.-J. Choi, J.-H. Choy, Nanomedicine 6 (2011) 803–814.
[47] H.-E. Chung, D.-H. Park, et al., Appl. Clay Sci. 65–66 (2012) 24–30.
[48] M. Chen, H.M. Cooper, et al., J. Colloid Interface Sci. 390 (2013) 275–281.
[49] H. Dong, M. Chen, et al., Appl. Clay Sci. (2014).
[50] S. Li, J. Li, et al., J. Mater. Chem. B 1 (2013) 61–68.
[51] S.-H. Wang, C.-W. Lee, et al., J. Nanobiotechnol. 8 (2010). pp. 33–33.
[52] C. He, Y. Hu, et al., Biomaterials 31 (2010) 3657–3666.
[53] Z.P. Xu, G. Stevenson, et al., J. Phys. Chem. B 110 (2006) 16923–16929.
[54] Y. Wong, K. Markham, et al., Biomaterials 31 (2010) 8770–8779.
[55] A. Li, L. Qin, et al., Biomaterials 31 (2010) 748–756.
[56] P.O. Andersson, C. Lejon, et al., Small 7 (2011) 514–523.
[57] N. Shah, R.J. Steptoe, et al., J. Pept. Sci. 17 (2011) 470–478.
[58] Z.P. Xu, M. Niebert, et al., J. Controlled Release 130 (2008) 86–94.
[59] Y.Y. Wong, H.M. Cooper, et al., J. Colloid Interface Sci. 369 (2012) 453–459.
[60] K.S. Matlin, H. Reggio, et al., J. Mol. Biol. 156 (1982) 609–631.
[61] W.T. Godbey, K.K. Wu, et al., Proc. Natl. Acad. Sci. USA 96 (1999) 5177–5181.
[62] I.S. Zuhorn, R. Kalicharan, et al., J. Biol. Chem. 277 (2002) 18021–18028.
[63] A. Elbakry, E.-C. Wurster, et al., Small 8 (2012) 3847–3856.
[64] M. Ogris, P. Steinlein, et al., AAPS Pharmsci 3 (2001). pp. E21–E21.
[65] S. Prabha, W.Z. Zhou, et al., Int. J. Pharm. 244 (2002) 105–115.
[66] S. Mayor, R.E. Pagano, Nat. Rev. Mol. Cell Biol. 8 (2007) 603–612.
[67] A. Vollrath, A. Schallon, et al., Soft Matter 9 (2013) 99–108.
[68] V. Cebrián, F. Martín-Saavedra, et al., Acta Biomater. 7 (2011) 3645–3655.